

MATHEMATICAL MODEL FOR FREEZING AND MELTING OF A NONREACTIVE BATH MATERIAL AROUND A LOW MELTING TEMPERATURE CYLINDRICAL SOLID ADDITIVE IN AN ADDITIVE-BATH SYSTEM

¹R.V.S. College of Engineering and Technology, Jamshedpur, INDIA

²National Institute of Technology, Jamshedpur, INDIA

³Birla Institute of Technology, Mesra, Ranchi, INDIA

Abstract: The intent of the present work is to devise a non-dimensional mathematical model of the integral format for unavoidable freezing and melting of nonreactive bath material onto a low melting temperature cylindrical additive of comparable thermal resistance with that of the bath including the frozen layer and heating and melting of the additive. It exhibits the event dependence on independent parameters: namely bath condition denoted by modified conduction factor, C_{ofm} , the phase-change parameters, the Stefan number of the additive, S_{ta} , and that of the bath material, S_{tb} , the thermo-physical property-ratio, γ , the heat-capacity ratio, C_r and the melt temperature-ratio of the additive bath system, θ_{ab} . Series solutions for small times and numerical solutions for all times of this event are obtained. These solutions are presented in graphical forms which reveal that reducing any one of C_{ofm} , S_{tb} , S_{ta} , and C_r and increasing either γ or θ_{ab} , decreases the total time of this event and consequently, increases the productivity. The solutions of these are obtained in closed forms. This problem is also validated by converting it to only convective heating of the additive.

Keywords: alloyant addition, additive-melt bath system, mathematical modelling, freezing and melting

1. INTRODUCTION

Due to tough competition in the global market, steel and cast iron of different grades need to be produced at low cost, with increased productivity, reduce energy consumption and environment impact but without degrading their quality. In manufacturing, their melt is first prepared by adding and assimilating alloying material, called additives, in the nonreactive hot melt bath which indicates that it does not react with the additive. It undergoes various metallurgical treatments before it is cast. In the melt preparation, however, unavoidable freezing and melting of the nonreactive bath material around the additive soon after dunking it in the bath, which is not required in the melt preparation, takes place. This event occurrence is due to the development of large temperature gradient towards the additive side soon after immersing it in the bath. It requires conductive heat much more than the bath convective heat. For thermal equilibrium, the excess of the conductive heat is compensated by the latent heat of fusion generated due to freezing of the bath material around the additive. As the time of immersion passes, the temperature gradient on the additive side decreases so much that the conductive heat requirement gets balanced by the bath convective heat with no further growth of the frozen layer.

Beyond this time, the temperature gradient on the additive side continues to decrease reducing the associated conductive heat. In this situation, the bath convective heat becomes larger than the conductive heat permitting the excess convective heat to melt the frozen layer till it completely melts exposing the low melting temperature additive in heated and molten condition. The molten portion immediately detaches and assimilates in the bath. This event takes certain time and increases the production time, cost, energy consumption and environment effect. In view of this, it is essential to reduce these by diminishing the time of this event for making the product globally competitive. Since the freezing and melting depends upon the size and shape of the additive, the temperature of the additive and that of the bath, the thermo-physical properties of the additive-bath system and condition of the bath, regulating these suitably provides desired reduction in time of the freezing and melting and, in turn, the production time. As it is a complex event, it can be estimated only by resorting to develop its suitable mathematical model.

Such a study for low melting temperature cylindrical additive having its thermal resistance comparable with that of the bath material including the frozen layer seldom appears in the literature. Nevertheless, the freezing and melting of the bath material onto high melting additives was investigated, for plate [1,2]*, cylindrical [3-10] and spherical [11-19] additives. It was reported that reducing the freezing temperature of the bath material or increasing the bath convective heat by raising the bath convective heat transfer diminishes the frozen layer thickness developed and the time of the freezing and melting for the plate [1], ferro-alloy cylinder dissolution [3] in hot metal steel bath and spherical [12] in the liquid bath. Further, for the cylinder of titanium [6-8], zirconium [9] and niobium [11], and the aluminum sphere in the salt melt bath [20], decreasing their diameter reduces the time of freezing and melting.

This time was also found for the frozen layer grown of negligible thermal resistance with respect to that of the sphere made of ferro-manganese [21]. For the frozen layer thickness developed of negligible thermal resistance with that of the high melting temperature, sponge iron sphere [22], cylinder [23] and plate [24], the close-form solutions for the freezing and melting were reported. The freezing and melting was also analyzed in case of the cylindrical additive of negligible thermal resistance [25] with respect to that of the bath including the frozen layer. The instant interface temperature between the cylindrical additive of high [26] or low [27] melting temperature and between the high melting temperature plate [28] immediately after their immersion in the bath was derived in close-forms. The effect of temperature dependent heat – capacity of the plate was also obtained on the freezing and melting of bath material with [29] and without agitation [30] of the bath onto the plate when the thermal resistance of the frozen layer thickness of the plate was negligible.

The present study relates to the undesirable freezing and melting of the bath material onto a low melting temperature cylindrical additive that takes place immediately after its immersion in the bath and the associated heating and melting of the additive. The thermal resistance offered by the additive is assumed to be comparable with that of the bath including the frozen layer. Its mathematical model of non-dimensional integral form is developed giving its control by non-dimensional independent parameters; namely the property-ratio, γ , the temperature-ratio, Θ_{ab} , the heat capacity-ratio, C_r of the additive bath-system, the bath condition represented by the conduction factor, C_{of} , the phase-change parameters, the Stefan number of the additive, S_{ta} and that of the bath material, S_{tb} . Series solutions for short times and numerical solutions for all times are obtained for this event of the freezing and melting and the associated heating and the melting of the additive. Additionally, closed-form solutions for limiting cases of $\gamma \rightarrow \infty$ and $\gamma \rightarrow 0$, $S_{ta} \rightarrow 0$, $S_{ta} \rightarrow \infty$, and $S_{tb} \rightarrow 0$ and $S_{tb} \rightarrow \infty$ are derived. This problem is also validated by transforming it to that of the additive subjected to bath convective heating

N.B.: * number in the parenthesis indicates the reference number

2. MATHEMATICAL MODEL

Consider a low melting temperature cylindrical additive of radius r_a . It is immersed at an initial uniform temperature T_{ai} in a hot nonreactive melt bath maintained at a constant temperature T_b higher than its freezing temperature T_{bm} . Instantly, the freezing of the bath material onto the additive commences, the interface formed between the freezing layer and the additive arrives at a temperature T_e that resides between the initial temperature T_{ai} of the additive and the freezing temperature, T_{bm} of the bath material, and the melting of the additive along with heating of the additive sets in. Due to this, a temperature field, $T_b > T_{bm} > T_e > T_{am} > T_{ai}$ established in the additive-bath system, Figure 1.

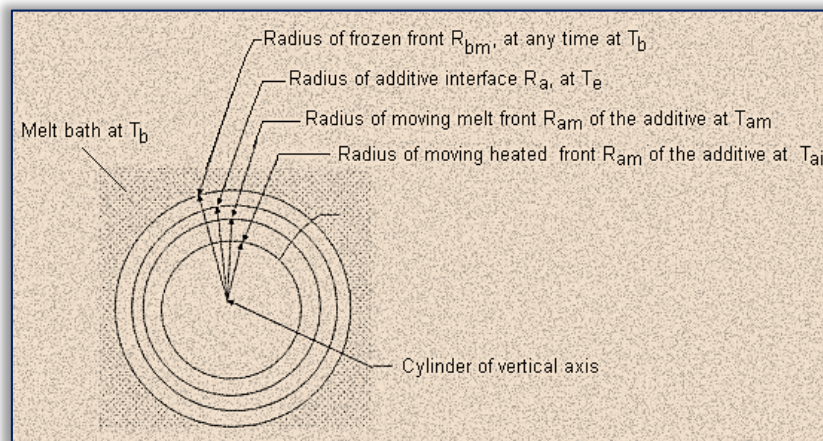


Figure-1: Diagram exhibiting freezing and melting of bath material onto the low melting temperature cylindrical solid additive of comparable thermal resistance with that of the additive.

With passing of the time, the frozen layer grows in thickness to its maximum extent and then melts completely. During this time, the temperature of the interface rises to the freezing temperature of the bath material, and the melt depth and the heat penetration depth of the additive increase. The occurrence of this event is due to the fact that as soon as the additive is plunged in the bath, a far greater temperature gradient on the additive side than that of the bath side is developed causing the conductive heat requirement by the additive much more than the convective heat available from the bath resulting in balancing of the excess conductive heat by

the latent heat of fusion generated owing to the freezing of the bath material around the additive. Elapsing time reduces the temperature gradient onto the additive side and, in turn, the conductive heat requirement until it becomes equal to the bath convective heat. Beyond this time, the convective heat becomes greater than the conductive heat needed by the additive. It results in the melting of the frozen layer till it melts completely. In this entire period, the interface temperature rises and the melt depth and heat penetration depth of the additive increase.

The events of freezing and melting, melting and heating of the additive are axi-symmetric and conduction-controlled. Each of these events can be governed by integral form of transient heat conduction equation. The freezing and melting is represented by

$$\left[\frac{d}{d\tau} \int_{C_r}^{R_{bm}} R_{bf} \theta_{bf} dR_{bf} - [R_{bf} \theta_{bf}]_{R_{bf}=R_{bm}} \frac{dR_{bm}}{d\tau} + [R_{bf} \theta_{bf}]_{R_{bf}=C_r} \frac{dC_r}{d\tau} \right] = R_{bf} \frac{\partial \theta_{bf}}{\partial R_{bf}} \Big|_{R_{bf}=R_{bm}} - R_{bf} \frac{\partial \theta_{bf}}{\partial R_{bf}} \Big|_{R_{bf}=C_r},$$

$$C_r \leq R_{bf} \leq R_{bm}, \tau > 0 \quad (1)$$

It is subjected to the initial and boundary conditions

$$\theta_{bf} = \theta_b, C_r \leq R_{bf} \leq R_{bm}, \tau = 0 \quad (2)$$

$$\theta_{bf} = \theta_e > \theta_{ab}, R_{bf} = C_r, \tau > 0 \quad (3)$$

$$\frac{\partial \theta_{bf}}{\partial R_{bf}} = \frac{1}{S_{tb}} \frac{dR_{bf}}{d\tau} + \frac{1}{C_{ofm}}, \theta_{bf} = 1, R_{bf} = R_{bm}, \tau > 0 \quad (4)$$

The melting of the additive is given by

$$\gamma \left[\frac{d}{d\tau} \int_{R_{am}}^1 R_{af} \theta_{af} dR_{af} - [R_{af} \theta_{af}]_{R_{af}=1} \frac{d1}{d\tau} + [R_{af} \theta_{af}]_{R_{af}=R_{am}} \frac{dR_{am}}{d\tau} \right] = R_{af} \frac{\partial \theta_{af}}{\partial R_{af}} \Big|_{R_{af}=1} - \frac{\partial \theta_{af}}{\partial R_{af}} \Big|_{R_{af}=R_{am}} \quad (5)$$

Its related initial and boundary conditions are

$$\theta_{af} = 0, 0 \leq R_{af} \leq 1, \tau = 0 \quad (6)$$

$$\theta_{af} = \theta_e > \theta_{ab}, R_{af} = 1, \tau > 0 \quad (7)$$

$$\theta_{af} = \theta_{ab}, R_{af} = R_{am}, \tau > 0 \quad (8)$$

The heating of the additive is regulated by

$$\gamma \left[\frac{d}{d\tau} \int_{R_{ai}}^{R_{am}} R_{ah} \theta_{ah} dR_{ah} - [R_{ah} \theta_{ah}]_{R_{ah}=R_{am}} \frac{dR_{am}}{d\tau} + [R_{ah} \theta_{ah}]_{R_{ah}=R_{ai}} \frac{dR_{ai}}{d\tau} \right] = R_{ah} \frac{\partial \theta_{ah}}{\partial R_{ah}} \Big|_{R_{ah}=R_{am}} - R_{ah} \frac{\partial \theta_{ah}}{\partial R_{ah}} \Big|_{R_{ah}=R_{ai}} \quad (9)$$

Initial and boundary condition concerning Eq (9) are

$$\theta_{ah} = 0, R_{ah} = 1, 0 \leq R_{ah} \leq 1, \tau = 0 \quad (10)$$

$$\theta_{ah} = \theta_{ab}, R_{ah} = R_{am}, \tau > 0 \quad (11)$$

$$\frac{\partial \theta_{ah}}{\partial R_{ah}} = 0, \theta_{ah} = 0, R_{ah} = R_{ai}, \tau > 0 \quad (12)$$

Coupling conditions at the interface between the melting layer and the frozen layer are cast as

$$\frac{1}{\gamma} \frac{\partial \theta_{af}}{\partial R_{af}} = \frac{\partial \theta_{bf}}{\partial R_{bf}}, \theta_{af} = \theta_{bf} = \theta_e > \theta_{ab}, R_{bf} = C_r, R_{af} = 1, \tau > 1 \quad (13)$$

whereas the conditions that conjugate the interface between the melt layer and heated region of the additive take the following form

$$\frac{\partial \theta_{af}}{\partial R_{af}} + \gamma \frac{1}{S_{ta}} \frac{dR_{am}}{d\tau} = \frac{\partial \theta_{ah}}{\partial R_{ah}}; \theta_{af} = \theta_{ah} = \theta_{ab}, R_{af} = R_{ah} = R_{am}, \tau > 0 \quad (14)$$

Note that Eqs.(1) to (14) denote the mathematical model in integral format for the freezing and melting of the bath material onto a low melting temperature cylindrical additive along with heating and melting of the additive. This model is evolved based on the assumptions of the uniform and the same thermo-physical properties of the heated region and the melt part of the additive whereas the frozen layer of the bath material and the additive material have uniform but different thermo-physical properties. The additive is assumed not to react with the bath. The volume change of the additive is taken as zero during its melting and heating processes. The surface of the frozen layer is taken in perfect contact with the surface of the additive due to

negligible effect of the interfacial resistance varying from $1.9 \times 10^{-4} \text{ m}^2\text{sK} / \text{J}$ to $2.1 \times 10^{-4} \text{ m}^2\text{sK} / \text{J}$ [31] due to imperfect contact between them. Previous investigators [1–33] found that their solutions for analogous problems are accurate and realistic with the assumption of the perfect contact. Also, the melt layer of the low melting temperature additive remains within the frozen layer of the high melting temperature bath material until the frozen layer completely melts. The growth of the frozen layer is symmetric about the central axis of the additive [32].

3. SOLUTIONS

The integral form of model denoted by Eqs.(1) to (14) is nonlinear due to the appearance of the phase-change moving boundary of the freezing of the bath material onto the additive, Eq.(5) and the melting of the additive Eq.(14) and coupled as a result of conjugating conditions at the interface between the melt layer of the additive and the frozen layer of the bath material onto additive, Eq.(13) and between the heated region and the melt layer of the additive, Eq.(17). These two features forbid to give exact solutions of the current problem applying available analytical methods of the literature. In such a case, semi-analytical techniques become important. One of these known as the integral method that provided closed-form solutions for several heating and phase change problems [36–38] in the previous studies is applied. Eq.(1) for the freezing and melting of the bath material onto the additive has already been written in integral format. Using Eqs.(3) and (4) it is reduced to

$$\left[\frac{d}{d\tau} \int_{C_r}^{R_{bm}} R_{bf} \theta_{bf} dR_{bf} - R_{bm} \frac{dR_{bm}}{d\tau} \right] = R_{bf} \frac{\partial \theta_{bf}}{\partial R_{bf}} \Big|_{R_{bf}=R_{bm}} - R_{bf} \frac{\partial \theta_{bf}}{\partial R_{bf}} \Big|_{R_{bf}=C_r} \quad (15)$$

whereas the integral Eq.(5) for the melting of the additive is simplified to

$$\gamma \left[\frac{d}{d\tau} \int_{R_{af}}^1 \theta_{af} R_{af} dR_{af} + \theta_{ab} R_{am} \frac{dR_{am}}{d\tau} \right] = R_{af} \frac{\partial \theta_{af}}{\partial R_{af}} \Big|_{R_{af}=1} - R_{af} \frac{\partial \theta_{af}}{\partial R_{af}} \Big|_{R_{af}=R_{am}} \quad (16)$$

once Eqs.(7) and (8) are substituted, The integral Eq.(9) for the heating of the additive assumes the following format

$$\gamma \left[\frac{d}{d\tau} \int_{R_{ai}}^{R_{am}} \theta_{ah} R_{ah} dR_{ah} - \theta_{ab} R_{am} \frac{dR_{am}}{d\tau} \right] = R_{ah} \frac{\partial \theta_{ah}}{\partial R_{ah}} \Big|_{R_{ah}=R_{am}} - R_{ah} \frac{\partial \theta_{ah}}{\partial R_{ah}} \Big|_{R_{ah}=R_{ai}} \quad (17)$$

after the application of Eqs.(12) to it.

For facilitating solutions, Eqs.(16) and (17) are added. The resultant equation, called global integral equation becomes

$$\gamma \left[\frac{d}{d\tau} \int_{R_{ai}}^{R_{am}} \theta_{ah} R_{ah} dR_{ah} + \frac{d}{d\tau} \int_{R_{af}}^1 \theta_{af} R_{af} dR_{af} \right] = R_{af} \frac{\partial \theta_{af}}{\partial R_{af}} \Big|_{R_{af}=1} + \frac{\gamma}{S_{ta}} R_{am} \frac{dR_{am}}{d\tau} \quad (18)$$

if Eqs.(12) and (14) are applied. To obtain the solutions of these integral equations, Eqs.(15) and (18), temperature distribution in each of the freezing layer, heating and melting regions of the additive need to be prescribed. In the frozen layer a linear temperature profile of the type

$$\theta_{bf} = \theta_e + (1-\theta_e) \left(\frac{R_{bf} - C_r}{R_{bm} - C_r} \right) \quad (19)$$

a cubic temperature distribution of the following format in the heated region of the additive

$$\theta_{ah} = \theta_{ab} \left(\frac{R_{ah} - R_{ai}}{R_{am} - R_{ai}} \right)^3 \quad (20)$$

and a linear temperature distribution in the melting layer

$$\theta_{af} = \theta_e - (\theta_e - \theta_{ab}) \left(\frac{1 - R_{af}}{1 - R_{am}} \right) \quad (21)$$

are assumed. Note that Eq.(19) satisfies the boundary conditions, Eqs.(3) and (4), Eq.(20) fulfills the boundary conditions, Eqs.(11) and (12) and Eq.(21) is compatible with the boundary conditions, Eqs.(7) and (8). Moreover, the cubic temperature profile Eq.(20) in the heating problem [35,36] yielded results which are closed to exact solution [37], whereas a linear profile Eq.(19) for freezing [1,26–28] and Eq.(21) for melting [34,38–40] of the additive provide accurate results. Substitution of Eqs. (4) and (19) in Eq.(15) leads to

$$\frac{d}{d\tau} \left[\frac{\theta_e}{2} (R_{bm}^2 - C_r^2) + (1 - \theta_e) \left\{ \frac{1}{2} R_{bm} (R_{bm} - C_r) - \frac{1}{6} (R_{bm} - C_r)^2 \right\} - \frac{R_{bm}^2}{2} \right] = \frac{R_{bm}}{C_{ofm}} + \frac{R_{bm}}{S_{ib}} \frac{dR_{bm}}{d\tau} + \frac{C_r (\theta_e - 1)}{R_{bm} - C_r} \quad (22)$$

whereas application of Eqs.(20) and (21) to Eq.(18) gives

$$\gamma \frac{d}{d\tau} \left[\theta_{ab} \left\{ \frac{R_{am}}{4} (R_{am} - R_{ai}) - \frac{1}{20} (R_{am} - R_{ai})^2 \right\} + \frac{\theta_e}{2} (1 - R_{am})^2 - (\theta_e - \theta_{ab}) \left\{ \frac{R_{am}}{2} (1 - R_{am}) + \frac{1}{6} (1 - R_{am})^2 \right\} + \frac{R_{am}^2}{2S_{ia}} \right] = \frac{\theta_e - \theta_{ab}}{1 - R_{am}} \quad (23)$$

Employing Eqs.(19) and (20) , conjugating condition Eq.(13) at the interface between the melt layer of the additive and the frozen layer of the bath onto the additive takes the form

$$\frac{\theta_e - \theta_{ab}}{1 - R_{am}} = \frac{\gamma(1 - \theta_e)}{R_{bm} - C_r} \quad (24)$$

whereas, the coupling condition between the melt layer and heated interface of the additive, Eq.(18) becomes

$$\frac{\theta_e - \theta_{ab}}{1 - R_{am}} + \frac{\gamma}{S_{ia}} \frac{dR_{am}}{d\tau} = \frac{3\theta_{ab}}{R_{am} - R_{ai}} \quad (25)$$

when Eqs. (20) and (21) are applied to it.

It is noted that as these four equations, Eqs (22) to (25) are in terms of four unknown variables, R_{ai} , R_{am} , R_{bm} and θ_e . they yield unique solutions but do not give closed-form solutions for them due to the presence of $dR_{am}/d\tau$ in Eq.(25). To overcome this difficulty, $dR_{am}/d\tau$ is converted to an algebraic expression by using the property of θ_{ab} , which is constant, at the phase-change interface $R_{af} = R_{am}$, $\Delta\theta_{af} = \Delta\theta_{ab} = 0$

$$\theta_{af} = \theta_{af} [R_{af}(\tau), \tau] \quad (26)$$

$$\Delta\theta_{af} = \frac{\partial\theta_{af}}{\partial R_{af}} \frac{dR_{af}}{d\tau} + \frac{\partial\theta_{af}}{\partial\tau} = 0 \quad (27)$$

Using the differential form of Eq(5) along with Eq (21). In Eq(27) gives

$$\frac{dR_{am}}{d\tau} = \frac{-1}{\gamma R_{am}} \quad (28)$$

Using Eq. (28) converts Eq. (25) to

$$\frac{\theta_e - \theta_{ab}}{1 - R_{am}} + \frac{1}{S_{ia} R_{am}} = \frac{3\theta_{ab}}{R_{am} - R_{ai}} \quad (29)$$

it gives

$$\frac{3\theta_{ab}}{R_{am} - R_{ai}} = \frac{S_{ia} (\theta_e - \theta_{ab}) R_{am} - (1 - R_{am})}{S_{ia} R_{am} (1 - R_{am})} \quad (30)$$

Substitution of Eq. (30) in Eq.(23) provides

$$\frac{d}{d\tau} \left[\frac{A}{4} \frac{R_{am}^2 (1 - R_{am})}{BR_{am} - (1 - R_{am})} - \frac{C}{20} \left\{ \frac{R_{am} (1 - R_{am})}{BR_{am} - (1 - R_{am})} \right\}^2 + \frac{\theta_e}{2} (1 - R_{am})^2 - (\theta_e - \theta_{ab}) R_1 + \frac{R_{am}^2}{2S_{ia}} \right] = \frac{(\theta_e - \theta_{ab})}{\gamma(1 - R_{am})} \quad (31)$$

where, $A=3\theta_{ab}^2 S_{ia}$, $B=S_{ia}(\theta_e - \theta_{ab})$ and $C=9\theta_{ab}^3 S_{ia}^2$, $R_1 = \frac{1}{2} R_{am} (1 - R_{am}) + \frac{1}{6} (1 - R_{am})^2$

Application of Eq.(24) changes Eq.(22) to

$$\frac{d}{d\tau} \left[\frac{R_2 (R_{bm}^2 - C_r^2)}{R_3} + \frac{(1 - \theta_{ab})(R_{bm} - C_r) R_4}{R_3} - \frac{1}{2} \left(1 + \frac{1}{S_{ib}} \right) R_{bm}^2 \right] = \frac{R_{bm}}{C_{ofm}} - \frac{C_r (1 - \theta_{ab})}{R_3} \quad (32)$$

here , $R_2 = \theta_{ab} (R_{bm} - C_r) + \gamma(1 - R_{am})$, $R_3 = (R_{bm} - C_r) + \gamma(1 - R_{am})$, $R_4 = \frac{1}{2} R_{bm} (R_{bm} - C_r) - \frac{1}{6} (R_{bm} - C_r)^2$.

Further use of Eq.(24) transforms Eq.(31) to

$$\frac{d}{d\tau} \left[\frac{R_{am}^2 R_2}{\gamma D R_{am} - R_3} - \frac{C}{20} \left(\frac{R_2 R_{am}}{\gamma D R_{am} - R_3} \right)^2 + \frac{R_2}{R_3} (1 - R_{am})^2 - \frac{\gamma(1 - \theta_{ab})(1 - R_{am}) R_1}{R_3} + \frac{R_{am}^2}{2S_{ia}} \right] = \frac{(1 - \theta_{ab})}{R_3} \quad (33)$$

where, $D=S_{ia}(1 - \theta_{ab})$,

Note that Eqs.(32) and (33) are in terms of two unknown variables R_{bm} and R_{am} . They readily give solutions subject to initial conditions $\tau=0$, $R_{bm} = C_r$ and $R_{am} = 1$. In terms of $dR_{bm}/d\tau$ and $dR_{am}/d\tau$. Eq. (32) becomes

$$a_{11} \frac{dR_{bm}}{d\tau} + a_{12} \frac{dR_{am}}{d\tau} = a_{13} \quad (34)$$

where,

$$\begin{aligned} a_{11} &= c_{11} + c_{12} + c_{13} + c_{14} + c_{15} + c_{16} - c_{17} - c_{18}; \quad a_{12} = d_{11} - d_{12} + d_{13}; \quad a_{13} = e_{11} - e_{12}. \\ c_{11} &= R_2 R_{bm} / R_3, \quad c_{12} = \theta_{ab} (R_{bm}^2 - C_r^2) / 2R_3, \quad c_{13} = R_2 (R_{bm}^2 - C_r^2) / 2R_3^2, \quad c_{14} = (1 - \theta_{ab}) R_{bm} (R_{bm}^2 - C_r^2) / 2R_3, \\ c_{15} &= (1 - \theta_{ab}) (R_{bm} - C_r)^2 / 6R_3, \quad c_{16} = (1 - \theta_{ab}) R_4 / R_3, \quad c_{17} = (1 - \theta_{ab}) R_4 (R_{bm} - C_r) / R_3^2, \\ c_{18} &= (1 + S_{tb}) R_{bm} / S_{tb} R_3^2. \\ d_{11} &= R_2 \gamma (R_{bm}^2 - C_r^2) / 2R_3^2, \quad d_{12} = \gamma (R_{bm}^2 - C_r^2) / 2R_3, \quad d_{13} = \gamma (1 - \theta_{ab}) R_4 (R_{bm} - C_r) / R_3^2, \\ e_{11} &= R_{bm} / C_{ofm}, \quad e_{12} = C_r (1 - \theta_{ab}) / R_3. \end{aligned}$$

and Eq.(33) assumes the following form

$$a_{21} \frac{dR_{bm}}{d\tau} + a_{22} \frac{dR_{am}}{d\tau} = a_{23} \quad (35)$$

Here,

$$\begin{aligned} a_{21} &= c_{21} - c_{22} - c_{23} + c_{24} - c_{25} - c_{26}, \quad a_{22} = d_{21} + d_{22} - d_{23} + d_{24} + d_{25} + d_{26} - d_{27} - d_{28} - d_{29} + d_{30} + d_{31} + d_{32} + d_{33}. \\ a_{23} &= \frac{(1 - \theta_{ab})}{R_3} \end{aligned}$$

with

$$\begin{aligned} c_{21} &= \frac{AD\gamma R_{am}^4}{4(\gamma DR_{am} - R_3)^2}, \quad c_{22} = \frac{CD R_3^2 R_{am}^3}{10(\gamma DR_{am} - R_3)^2}, \quad c_{23} = \frac{CD\gamma R_3^2 R_{am}^3 (D+1)}{10(\gamma DR_{am} - R_3)^3}, \quad c_{24} = \frac{\theta_{ab} (1 - R_{am}^2)}{2R_3}, \quad c_{25} = \frac{R_2 (1 - R_{am}^2)}{2R_3^2}, \\ c_{26} &= \frac{\gamma (1 - \theta_{ab}) R_1 (1 - R_{am})}{R_3^2}, \quad d_{21} = \frac{AR_3 R_{am}}{2(\gamma DR_{am} - R_3)}, \quad d_{22} = \frac{A\gamma R_{am}^2}{4(\gamma DR_{am} - R_3)}, \quad d_{23} = \frac{A(D+1)\gamma R_{am}^2}{4(\gamma DR_{am} - R_3)^2}, \quad d_{24} = \frac{CR_3^2 R_{am} (1 - \gamma)}{10(\gamma DR_{am} - R_3)^2}, \\ d_{25} &= \frac{R_3^2 R_{am}^2 \gamma (D+1)}{10(\gamma DR_{am} - R_3)^3}, \quad d_{26} = \frac{R_2 R_{am}}{R_3}, \quad d_{27} = \frac{\gamma (1 - R_{am}^2)}{2R_3}, \quad d_{28} = \frac{R_2 \gamma (1 - R_{am}^2)}{2R_3^2}, \quad d_{29} = \frac{\gamma (1 - \theta_{ab}) (1 - R_{am})^2}{6R_3}, \\ d_{30} &= \frac{\gamma (1 - \theta_{ab}) R_{am} (1 - R_{am})}{R_3}, \quad d_{31} = \frac{\gamma (1 - \theta_{ab}) R_1}{R_3}, \quad d_{32} = \frac{\gamma^2 (1 - \theta_{ab}) R_1 (1 - R_{am})}{R_3^2}, \quad d_{34} = \frac{R_{am}}{S_{ta}}. \end{aligned}$$

Eqs.(34) and (35) provide

$$\frac{dR_{bm}}{d\tau} = \frac{a_{12} a_{23} - a_{13} a_{22}}{a_{12} a_{21} - a_{11} a_{22}} \quad (36)$$

$$\frac{dR_{am}}{d\tau} = \frac{a_{13} a_{21} - a_{23} a_{11}}{a_{12} a_{21} - a_{11} a_{22}} \quad (37)$$

Eqs.(36) and (37) are simultaneous first order ordinary differential equations in an independent variable time and form an initial value problem with initial conditions $R_{bm}=C_r$, $R_{am}=1$ at $\tau = 0$. They do not give closed form solutions but provide numerical solutions, when the Runge-Kutta method is applied. However, the solutions do not get started owing to yielding ∞ or $0/0$ values at the initial conditions. To overcome this difficulty series solutions for small times are obtained. From these starting values of R_{bm} , R_{am} and θ_e in the vicinity of $\tau \rightarrow 0$ ($\tau=10^{-4}$) are found. Applying these, the Runge-Kutta method gets started due to which subsequent values of R_{bm} and R_{am} are obtained using the computer software MATLAB of the Runge-Kutta method. The corresponding value of θ_e from Eq(24) and heat penetration depth R_{ai} from Eq(30) are then derived.

Once the interface temperature, θ_e , rises to the freezing temperature of the bath material ($\theta_e=1$), it becomes equal to the temperature at the freezing front of the bath material. At this juncture, the entire frozen layer becomes at the freezing temperature of the bath material with no temperature gradient along the frozen layer thickness. Due to this $\left(\frac{\partial \theta_{bf}}{\partial R_{bf}} = 0 \right)$, no further freezing takes place nor does heat penetrate in the additive. The

continued convective heat from the bath only melt the developed frozen layer. The application of the this fact in Eq.(4) leads to

$$\frac{1}{S_{tb}} \frac{dR_{bf}}{d\tau} + \frac{1}{C_{ofm}} = 0 \quad (38)$$

giving the close-form solution

$$R_{bm} = R_{bmx} - \frac{S_{tb}}{C_{ofm}}(\tau - \tau_{max}) \quad (39)$$

Eq.(39) satisfies the boundary condition $(\tau = \tau_{max})$ when $(R_{bm} = R_{bmx})$, the thickness of maximum frozen layer. It readily gives the total time, τ_t of freezing and melting, once R_{bmx} after melting of the frozen layer, becomes C_r . Their substitution in Eq.(38) gives

$$\tau_t = \frac{C_{ofm}}{S_{tb}} R_{bm}^* + \tau_{max} \quad (40)$$

where $R_{bm}^* = R_{bmx} - C_r$.

Note that the values R_{bmx} and R_{am} are obtained from the series solutions for small times.

4. SERIES SOLUTIONS FOR SMALL TIMES

Series Solutions satisfying the initial conditions at initial time $\tau = 0$, R_{bm} , R_{am} and θ_e are assumed, respectively, as

$$R_{bm} = \sum_{i=0}^n a_i \tau^{i/2} \quad (41)$$

$$R_{am} = \sum_{i=0}^n b_i \tau^{i/2} \quad (42)$$

$$\theta_e = \sum_{i=0}^n c_i \tau^{i/2} \quad i=0,1,2,\dots,n \quad (43)$$

They are directly used in Eq.(24), Eq.(33) and Eq.(34) rather than in Eqs.(24),(36) and (37) At the initial time $\tau = 0$, $R_{bm}=C_r$, $R_{am}=1$, Eqs.(40) and (41) provide $a_0 = C_r$, $b_0 = 1$, and other high order coefficients of τ i.e $\tau^{i/2}$. Using the first order coefficients a_1 and b_1 of Eqs.(41) and (42), zeroth order coefficient of c_0 , of Eq.(43) can be found.

$$c_0 = \frac{\theta_{ab} a_1 - \gamma b_1}{a_1 - \gamma b_1} \quad (43)$$

where,

$$a_1 = \left[\frac{D_3 \pm \sqrt{(D_3^2 - 4D_1 D_2)}}{2D_1 D_2} \right]^{1/2}, b_1 = \frac{A_1 a_1^2 - (1 - \theta_{ab})}{\gamma A_2 a_1}, A_1 = \frac{3}{4} \theta_{ab} + S_{tbm}, A_2 = \frac{3}{4} + S_{tbm}, B_1 = \frac{3}{4} \theta_{ab}^2,$$

$$B_2 = \frac{3}{2} \theta_{ab}^2 + \theta_{ab} (\theta_{ab} - 1) - \frac{(\theta_{ab} - 1)}{S_{ta}}, S_{tbm} = -\frac{1}{2} - \frac{1}{2S_{tb}}, B_4 = 2\gamma (\theta_{ab} - 1)^2, B_3 = -\frac{3}{4} \theta_{ab}^2 - (\theta_{ab} - 1) - \frac{1}{2} (\theta_{ab} - 1)^2 + \frac{(\theta_{ab} - 1)}{S_{ta}},$$

$$C_1 = -B_1 + B_2 \frac{A_1}{A_2}, C_2 = B_4 + \frac{B_2 (\theta_{ab} - 1)}{A_2}, D_1 = C_1 + B_3 \frac{A_1^2}{A_2^2}, D_2 = \frac{B_3^2}{A_2^2} (\theta_{ab} - 1)^2, D_3 = C_2 + \frac{2A_1 B_3 (\theta_{ab} - 1)}{A_2^2}$$

5. LIMITING CASES

— Case I, $\gamma = 0$, $0 \leq S_{tb} \leq \infty$, $0 \leq S_{ta} \leq \infty$ and $\theta_{ab} < 1$:

When the property – ratio of the additive – bath system, $\gamma \rightarrow 0$, the additive acts as infinite heat capacity material due to which, the additive temperature does not rise beyond its initial temperature even though a large amount of heat is conducted to it from the bath. In this situation, the additive acts as a thermal reservoir and no heating and melting of the additive takes place. It results in $1 - R_{am} = 0$, $R_{ai} = 1$ and $\theta_e = 0$. Application of these reduces Eq.(22) for freezing and melting to

$$\frac{d}{d\tau} \left[\left\{ \frac{1}{2} R_{bm} (R_{bm} - C_r) - \frac{1}{6} (R_{bm} - C_r)^2 \right\} - \frac{1}{2} \left(1 + \frac{1}{S_{tb}} \right) R_{bm}^2 \right] = \frac{R_{bm}}{C_{ofm}} - \frac{C_r}{R_{bm} - C_r} \quad (45)$$

After simplification it takes the form

$$\left[\frac{1}{6} (R_{bm} - C_r) - \left(\frac{1}{2} + \frac{2}{S_{tb}} \right) R_{bm} \right] \frac{dR_{bm}}{d\tau} = \left[\frac{R_{bm} (R_{bm} - C_r) - C_r C_{ofm}}{C_{ofm} (R_{bm} - C_r)} \right] \quad (46)$$

It gives the closed form solution

$$\tau = BR_{bm} - E \ln(R_{bm}^2 - C_r R_{bm} - C_r C_{ofm}) + F \ln \left(\frac{2R_{bm} - C_r - \sqrt{(C_r^2 + 4C_r C_{ofm})}}{2R_{bm} - C_r + \sqrt{(C_r^2 + 4C_r C_{ofm})}} \right) \quad (47)$$

satisfying the initial conditions $\tau=0$ and $R_{bm}=C_r$.

$$\text{Here, } A = \left(\frac{1}{2} + \frac{1}{S_{tb}} \right), B = \frac{C_{ofm}(1-A)}{6}, C = \frac{C_r C_{ofm}(2+A)}{6}, D = \frac{C_r^2 C_{ofm}}{6}, E = \frac{1}{2}(BC_r - C),$$

$$F = \left[\frac{B(C_r^2 - 2C_r C_{ofm})}{2} - \frac{CC_r}{2} + D \right] \frac{1}{\sqrt{C_r^2 + C_r C_{ofm}}}$$

— **Case II.** $\gamma \rightarrow \infty, 0 \leq S_{tb} \leq \infty, 0 \leq S_{ta} \leq \infty$ and $\theta_{ab} < 1$;

If the property – ratio of the additive – bath system is of infinite value ($\gamma \rightarrow \infty$) the additive acts as negligible heat capacity material. In this situation the interface temperature of the additive rises quickly to attain the freezing temperature of the bath material ($\theta_e = 1$) even a small amount of heat from the bath is supplied to the additive. $\gamma \rightarrow \infty$ is also achieved when the additive thermal conductivity $K_a \rightarrow 0$. It makes the additive a perfect insulator, due to which its thermal resistance becomes infinite which does not permit the bath convective heat to be conducted to the additive resulting in no freezing of the bath material onto the additive. Consequently, the event of freezing and melting does not occur.

— **Case III.** $S_{ta} \rightarrow 0, 0 \leq S_{tb} \leq \infty, 0 \leq \gamma \leq \infty$ and $\theta_{ab} < 1$;

Additive of infinite latent heat of fusion makes its Stefan number, $S_{ta} \rightarrow 0$. It needs very large amount of heat to melt which is not available from the combination of convective heat and latent heat of fusion due to freezing of the bath material onto the additive. This results in only heating of the additive. In this condition, the current problem becomes that of the freezing and melting of the bath material onto the high melting temperature additive investigated earlier [8].

— **Case IV.** $S_{ta} \rightarrow \infty, 0 \leq S_{tb} \leq \infty, 0 \leq \gamma \leq \infty$ and $\theta_{ab} < 1$;

It implies that the additive latent heat of fusion is of negligible value allowing the formation of large thickness of the melt of the additive for the same bath convective heat. Substituting

$S_{ta} \rightarrow \infty$ in Eq.(25) gives the interface temperature

$$\theta_e = \theta_{ab} + \frac{3\theta_{ab}(1 - R_{am})}{R_{am} - R_{ai}} \quad (48)$$

In finding the behavior of R_{bm}, R_{am} and R_{ai} with time. Eq.(48) is placed in Eqs.(36) and (37) along with $S_{ta} \rightarrow \infty$.

Case V. $S_{tb} \rightarrow 0, 0 \leq S_{ta} \leq \infty, 0 \leq \gamma \leq \infty$ and $\theta_{ab} < 1$:

$S_{tb} \rightarrow 0$ relates to the bath material of infinite latent heat of fusion ($L \rightarrow \infty$) due to which the freezing of the bath material generates large amount of heat which is conducted to the additive along with the bath convective heat to balance the requirement of the conductive heat of the bath. This heat raises the interface temperature to the freezing temperature of the bath material ($\theta_e \rightarrow 1$). Moreover, due to this feature of the bath material, a thin layer of the frozen bath material is developed. This event, therefore, transforms to the freezing and melting of an agitated bath material onto a low melting temperature cylindrical solid additive that was studied earlier [41] by the present authors.

— **Case VI.** $S_{tb} \rightarrow \infty, 0 \leq S_{ta} \leq \infty, 0 \leq \gamma \leq \infty$ and $\theta_{ab} < 1$;

$S_{tb} \rightarrow \infty$ provides negligible latent heat of fusion of the bath material ($L \rightarrow 0$), due to which it develops a large thickness of the frozen layer onto the additive making its thermal resistance much more than that of the additive and, in turn, the additive thermal resistance becomes negligible with respect to that of the frozen layer. This event then becomes the freezing and melting of the bath material onto a negligible thermal resistance of low melting temperature cylindrical solid additive. This situation was investigated earlier by the current authors [42].

6. VALIDATION

If the convective heat available from bath is high enough to balance the conductive heat requirement of the additive, no freezing of the bath material and melting of the additive take place. Here, the melting boundary radius $R_{am}=1, \theta_{ab}=\theta_e, \gamma = 1$ and the convective heat only heats the additive due to which both the surface temperature and the heat penetration depth of the additive increase with passing of time. Moreover, these vanish Eq.(15) of freezing and Eq. (16) of additive melting and Eq.(9) reduces to

$$\left[\frac{d}{d\tau} \int_{R_{ai}}^1 R_{ah} \theta_{ah} dR_{ah} \right] = R_{ah} \frac{\partial \theta_{ah}}{\partial R_{ah}} \Big|_{R_{ah}=1} - R_{ah} \frac{\partial \theta_{ah}}{\partial R_{ah}} \Big|_{R_{ah}=R_{ai}} \quad (49)$$

whereas the temperature distribution in the heated region of the additive Eq(20) becomes

$$\theta_{ah} = \theta_{ab} \left(\frac{R_{ah} - R_{ai}}{R_{am} - R_{ai}} \right)^3, \theta_{ab} = \theta_e \quad (50)$$

and associated initial and boundary conditions for Eq(49) are

$$\theta_{ah} = 0, \tau = 0, R_{ai} \leq R_{ah} \leq 1 \quad (51)$$

$$\theta_{ah} = \theta_e, \frac{\partial \theta_{ah}}{\partial R_{ah}} = B_i (\theta_b - \theta_e), R_{ah} = 1, \tau > 0 \quad (52)$$

$$\theta_{ah} = 0, \frac{\partial \theta_{ah}}{\partial R_{ah}} = 0, R_{ah} = R_{ai}, \tau > 0 \quad (53)$$

Application of Eqs(52) and (53) in Eq(49) provides

$$\frac{d}{d\tau} \left[\theta_e \left\{ \frac{(1-R_{ai})}{4} - \frac{(1-R_{ai})^2}{20} \right\} \right] = B_i (\theta_b - \theta_e) \quad (54)$$

Left hand side of Eq(54) is exactly the same as the left hand side of Eq(23) obtained in the present problem when Eq(52) is applied. As there is no melting layer of the additive the surface of the additive gets convectively heated by the bath which, in turn, converts Eq(4) to

$$\frac{\partial \theta_{ah}}{\partial R_{ah}} = B_i (\theta_b - \theta_e), R_{ah} = 1, \tau > 0 \quad (55)$$

and with this application right hand side of Eq.(23) also becomes the same as the right hand side of Eq(54), thus, validating the current problem.

7. RESULTS AND DISCUSSIONS

The non-dimensional integral model developed for the current problem indicated the problem dependence upon non-dimensional independent parameters : the bath convection denoted by the modified conduction factor, C_{ofm} , the additive-bath system thermal property - ratio, γ , the heat capacity-ratio, C_r , and the melting-temperature ratio θ_{ab} , the phase-change parameter, the Stefan number of the additive, S_{ta} and that of the bath, S_{tb} . Their values of a prescribed bath and various additives added in the bath are exhibited in Table 1.

Table 1.: Based on thermos-physical properties of liquid steel [32]

$T_b = 1873K(1600^\circ C)$, $T_{bm} = 1793K(1520^\circ C)$, $C_{pa} = 782J/KgK$, $L_a = 268576 J/Kg$, $K_{bm} = 29.3W/mK$, $\rho_{bm} = 7100Kg/m^3$, $S_{tb} = 4.367$, $\theta_b = 1.05$

Additive	Thermo-physical properties of low melting temperature cylindrical solid additive [32] [$T_a = 298K(25^\circ C)$, $r_o = 0.01m$]					Non-dimensional parameters				
	T_{am} $^\circ C$	C_{pa} J/KgK	ρ_a Kg/m ³	L_a KJ/Kg	K_a^* W/mK	S_{ta}	θ_{ab}	γ	C_r	C_{ofm}
Ferromanganese	1266	700	7200	534654	7.53	1.62	0.83	4.28	1.10	6.03
Ferrosilicon	1227	586	4460	908200	9.62	0.77	0.80	6.47	2.12	11.63
Silicomanganese	1216	628	5600	578783	6.28	1.29	0.79	7.36	1.57	8.65

$h = 10000 W/m^2K$. [6]

The Stefan number is the ratio of the sensible heat and latent heat of fusion of the phase change material. Its high value denotes low latent heat of fusion permitting the growth of a larger thickness of the frozen layer of the bath material around the additive or larger molten layer of the additive. The conduction factor, is the ratio of the heat conducted to the additive as a result of the difference between the temperature of the freezing of the bath material and the initial temperature of the additive and the bath convective heat. It ranges from 0 to ∞ , ($0 \leq C_{of} \leq \infty$). $C_{of} \rightarrow 0$, implies no conductive heat transfer to the additive resulting in no freezing of the bath material onto the additive $C_{of} \rightarrow 0$ can be also attained once the bath is made highly agitated. Due to this the heat transfer coefficient, h becomes extremely high ($h \rightarrow \infty$) and consequently, the bath convective heat, $h(T_b - T_{bm})$ becomes high enough to balance the conductive heat requirement of the additive due to which the freezing does not occur. $C_{of} \rightarrow \infty$ is indicative of no bath convective heat. In this case, the heat conducted

to the additive is met by only the latent heat of fusion liberated due to freezing of the bath material around the additive resulting in only freezing. These facts indicate that the time of unavoidable freezing and melting can be decreased to almost negligible value when C_{of} is reduced to almost zero value ($C_{of} \rightarrow 0$) for a bath-additive system. In practice, it is achieved once the bath is made highly agitated. The property-ratio, γ is effusivity $\rho_b C_{pb} K_b$ of the bath material divided by the effusivity, $\rho_a C_{pa} K_a$ of the additive and is indicative of the thermal force. Its high value provides high thermal force in the bath owing to which large heat is transferred to the additive resulting in high temperature θ_e at the interface. θ_{ab} is the ratio of the melting temperature of additive and that of the bath material. For the low melting temperature additive considered in the current study, $\theta_{ab} < 1$. It allows the heat conducted to the additive both melting and heating of the additive. C_r , the heat capacity-ratio is the ratio of the heat capacity of the bath material and that of the additive. Reducing C_r decreases the heat capacity of the bath material which, in turn, diminishes the S_{tb} of the bath and as described above, this reduces the growth of the frozen layer.

Figure 2 shows the time variant freezing and melting of the bath material R_{bm}^* onto the low melting temperature cylindrical additive, build-up of the interface temperature θ_e between the additive and the freezing layer and the associated heating and melting of the additive for different modified conduction factor, C_{ofm} . These graphs are for certain S_{ta} , S_{tb} , C_r , γ and θ_{ab} , whereas Fig-3 corresponds to these graphs for various Stefan numbers of the bath material, S_{tb} , in case of prescribed values of C_{ofm} , S_{ta} , C_r , γ and θ_{ab} . These graphs in Figure 4 are for different Stefan number S_{ta} , of the additives. They are plotted for particular values of C_{ofm} , S_{tb} , C_r , γ and θ_{ab} . Above graphs appeared in Figure 5 are for various property – ratio, γ of the additive – bath system. These are for certain S_{ta} , S_{tb} , C_{ofm} , C_r and θ_{ab} . Illustrated in Figure 6 are these graphs for different C_r but for prescribed values of C_{ofm} , S_{ta} , γ and θ_{ab} . These graphs are also contained in Figure 7 for various additive melt temperature – ratio, θ_{ab} . They are for certain C_{ofm} , S_{ta} , C_r and γ .

All these figures exhibit the common features. The freezing and melting, R_{bm}^* assumes a parabolic behaviour with faster increase in the frozen layer to reach its maximum value R_{bmx}^* . The associated interface temperature rises to the freezing temperature of the bath material ($\theta_e=1$). Due to this, the interface temperature, the entire frozen layer and the interface between the maximum frozen layer and the bath become at the freezing temperature of the bath material resulting in making it a lump. Continued bath convective heat only melts this frozen layer which is governed by Eq.(45). It gives this melting a linear behavior with elapse of time. The associated heat penetration depth and the melt depth in the additive increase nonlinearly but quickly. In the melting of the frozen layer regime, the heat penetration depth and the melt depth in the additive do not change rather they remain at their maximum values.

— Effect of conduction factor, C_{ofm} :

Figure 2 displays the behaviour of the freezing and melting of the bath material R_{bm}^* onto the additive, the temperature built-up θ_e at the interface between the additive and the freezing layer, the melting layer R_{am}^* and the heated thickness R_{ai}^* of the additive with elapse of time measured from the start of the freezing and melting event for various modified conduction factor, C_{ofm} . They are for prescribed values of θ_{ab} , S_{ta} , S_{tb} , C_r and γ . It is observed that decreasing C_{ofm} diminishes the growth of the maximum frozen layer R_{bmx}^* its time of growth, the total time of the freezing and melting and the time of the melting of the developed frozen layer R_{bmx}^* and increases both the melt layer R_{am}^* , and the heat penetration thickness R_{ai}^* in the additive and the interface temperature θ_e . Physically, they are realistic since decreasing C_{ofm} increases the convective heat transfer and because heat conducted to the additive is balanced by sum of bath convective heat and latent heat of fusion generated due to the freezing of bath material onto the additive, the requirement of the latent heat of fusion reduces due to which smaller thickness of the frozen layer developed, Figure 2. Moreover, this increased convection melts and heats larger thickness of the additive, Figure 2.

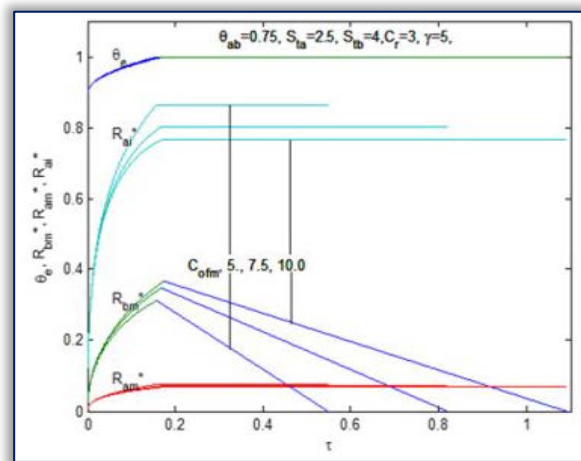


Figure-2: Time dependent freezing and melting of bath material R_{bm}^* onto the additive and corresponding melt depth, R_{am}^* , heat penetration depth R_{ai}^* and the interface temperature, θ_e , for different modified conduction factor, C_{ofm} . θ_{ab} , S_{ta} , S_{tb} , C_r and γ are taken as parameters.

— Influence of the Stefan number of the bath material, S_{tb} :

Figure 3 relates to the time dependent freezing and melting of the bath material onto the additive R_{bm}^* , the interface temperature, θ_e , the melt depth R_{am}^* and the heat penetration thickness, R_{ai}^* in the additive for different S_{tb} of the bath material. They are for prescribed values of θ_{ab} , S_{ta} , C_r , γ and C_{ofm} . Their features are similar to those described earlier, but for decreasing S_{tb} from 6 to 4 they reduce. They are correct because decrease in S_{tb} increases the latent heat of fusion owing to which a smaller thickness of the frozen layer is grown for the same convective heat supplied by the bath.

— Effect of the Stefan number of the additive, S_{ta} :

Figure 4 exhibits variation in the freezing and melting of the bath material, R_{bm}^* the interface temperature θ_e , the melt thickness, R_{am}^* and the heat penetration depth R_{ai}^* in the additive with time for various S_{ta} . They are plotted for certain θ_{ab} , S_{tb} , C_r , C_{ofm} and γ . Their behaviours are similar to those appeared in Figs.2 and 3. However, increasing S_{ta} of the additive from 2.5 to 3.5 has little effect on R_{bm}^* , R_{am}^* , θ_e in the freezing region of the bath material except R_{ai}^* that increases appreciably, whereas R_{am}^* and R_{ai}^* remain at their values in the melting region that are attained corresponding to R_{bm}^* . Physically, such behaviours are realistic because decreasing S_{ta} increases the latent heat of the fusion of additive and reduces the heat capacity of the additive resulting in development of smaller melt depth and larger heat penetration depth in the additive, Figure 4 for the same bath convective heat.

— Impact of Property-ratio of the additive-bath system, γ :

Figure 5 relates to time dependent freezing and melting of the bath material onto the additive, R_{bm}^* the interface temperature θ_e , the associated melt depth, R_{am}^* and the heat penetration depth R_{ai}^* in the additive for different values of property-ratio, γ . They are plotted for particular values of θ_{ab} , S_{ta} , S_{tb} , C_r , and C_{ofm} . Their features are similar to those exhibited in Figs.2,3,4. When γ increases, it diminishes the frozen layer thickness, R_{bm}^* , its time of growth τ_{max} and the total time of the freezing and melting τ_t , and increases both melt layer R_{am}^* and the heat penetration depth, R_{ai}^* , whereas interface temperature, θ_e remains almost unaffected. Physically, these predictions are realistic as increasing γ develops larger thermal force in the bath transferring large heat to the additive developing larger melt depth and heat penetration depth in the additive. Moreover, due to the increased thermal force of the bath less latent heat of fusion is needed to balance the conductive heat requirement of the additive. It builds up a smaller frozen layer thickness.

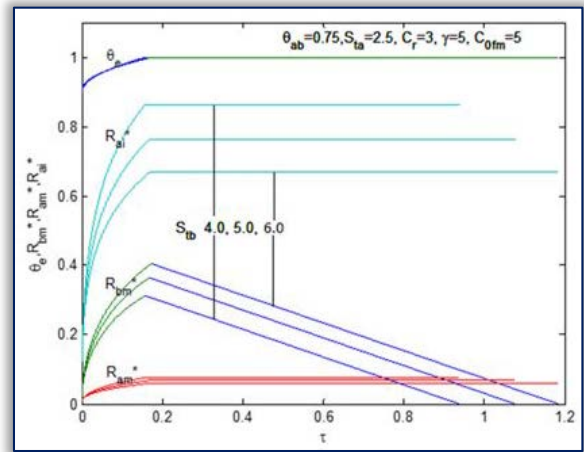


Figure-3: Time variant freezing and melting of bath material R_{bm}^* onto the additive and corresponding melt depth, R_{am}^* , heat penetration depth R_{ai}^* and the interface temperature, θ_e , for different Stefan number, S_{tb} of bath material. θ_{ab} , S_{ta} , C_r , C_{ofm} and γ are considered as parameters

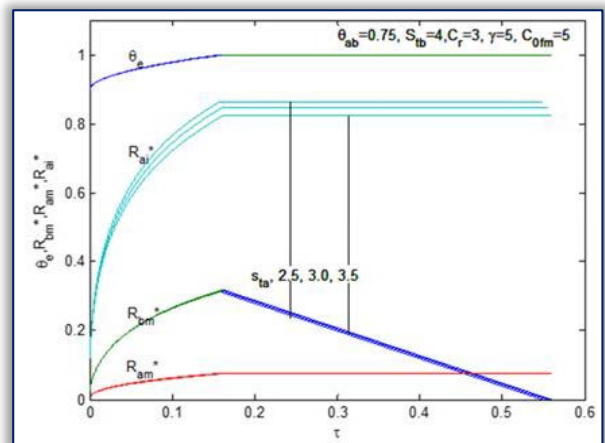


Figure-4: Behaviour of freezing and melting of bath material R_{bm}^* onto the additive and corresponding melt depth, R_{am}^* , heat penetration depth R_{ai}^* and the interface temperature, θ_e , with time for different Stefan number, S_{ta} of the additive. θ_{ab} , S_{tb} , C_r , C_{ofm} and γ are considered as parameters

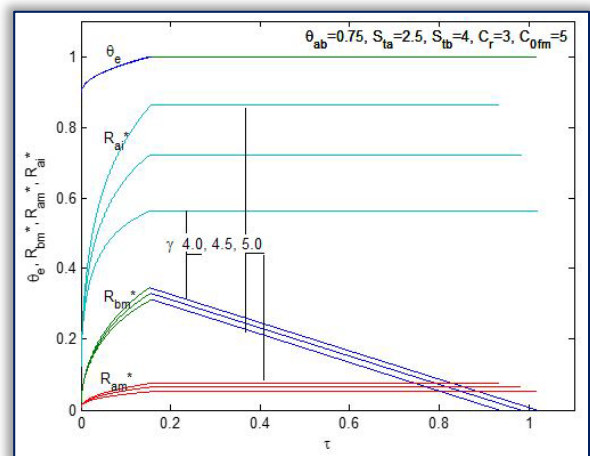


Figure-5: Effect of property-ratio, γ upon freezing and melting of bath material R_{bm}^* onto the additive and associated melt depth, R_{am}^* , of additive, heat penetration depth R_{ai}^* in the additive and the interface temperature, θ_e , with time, τ for certain values of θ_{ab} , S_{ta} , S_{tb} , C_r , and C_{ofm} .

— Effect of heat capacity-ratio, C_r :

Figure 6 corresponds to the time dependent growth of R_{bm}^* , build-up of interface temperature, θ_e , R_{am}^* and R_{ai}^* in the additive for different, C_r . These plots are for particular values of θ_{ab} , S_{ta} , S_{tb} , γ and C_{ofm} and their features are similar to those of Figs.2-5. They exhibit that increasing C_r increases the maximum frozen layer thickness, R_{bm}^* , its growth time, T_{max} , the total time of the freezing and melting of bath material, T_t but these increases are insignificant. From physical point of view, these predictions are true since decrease in C_r reduces the heat capacity of the frozen layer liberating less amount of sensible heat during freezing, resulting in availability of less total heat to be transferred to the additive, which is sum of the latent heat of fusion liberated and the release of sensible heat by the frozen layer plus the bath convective heat. It causes smaller rise of the interface temperature, θ_e and in turn, smaller temperature difference in the additive requiring less conductive heat which is compensated by growth of smaller frozen layer thickness as shown in the Figure 6.

— Impact of melting-temperature ratio, θ_{ab} :

Shown in Figure 7 are the time variant freezing and melting of the bath material onto the additive R_{bm}^* , the interface temperature θ_e , the melting depth, R_{am}^* and the heat penetration depth R_{ai}^* in the additive for different melt temperature-ratio, θ_{ab} . They are for given values of S_{ta} , S_{tb} , γ , C_r and C_{ofm} . Here also, their features are similar to those of Fig-6. Increasing θ_{ab} , decreases the growth of maximum frozen layer thickness, R_{bm}^* , its time of formation, T_{max} and the total time of the freezing and melting, T_t , the heat penetration depth, R_{ai}^* , and the melt depth, R_{am}^* . They are features are realistic because increasing θ_{ab} decreases the temperature difference in the additive, and in turn, reduces the conductive heat requirement due to which for the given convective heat of the bath, less latent heat of frozen is needed. It is achieved once a smaller frozen layer thickness grows, Figure 7.

8. CONCLUSIONS

Non-dimensional integral model evolved for the current problem states its controlled by independent non-dimensional parameters, the modified conduction factor, C_{ofm} , the Stefan number the bath material, S_{tb} , and that of the additive, S_{ta} , the thermo-physical property-ratio, γ , heat capacity - ratio, C_r , and the melt-temperature ratio, θ_{ab} , of the additive bath system. The model provides its series solutions for small times and numerical solutions for all times. Their graphical representations indicate that decreasing either each of the C_{ofm} , S_{tb} , S_{ta} , γ , C_r or increasing any of γ and θ_{ab} diminishes the time of the freezing and melting and, in turn, reduces the production time and increases the productivity making the product globally competitive.

The present problem is also validated by converting it to that of the convectively heated additive.

Nomenclature

- B_i Biot number, $hr0/Ka$
- B_{im} Modified Biot number, $(hr0/Ka)*(KaCa/KbCb)$
- C heat capacity (ρCp), $Jm^{-3} K^{-1}$
- K thermal conductivity, $Wm^{-1} K^{-1}$
- r radius, m

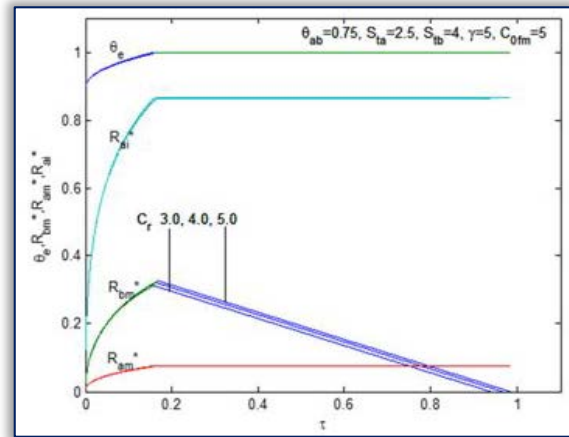


Figure-6: Time dependent freezing and melting of bath material R_{bm}^* , onto the additive and associated melt depth, R_{am}^* , of additive, heat penetration depth R_{ai}^* in the additive and the surface interface temperature, θ_e , for different values of capacity-ratio C_r , in case of particular values of θ_{ab} , S_{ta} , S_{tb} , γ and C_{ofm} .

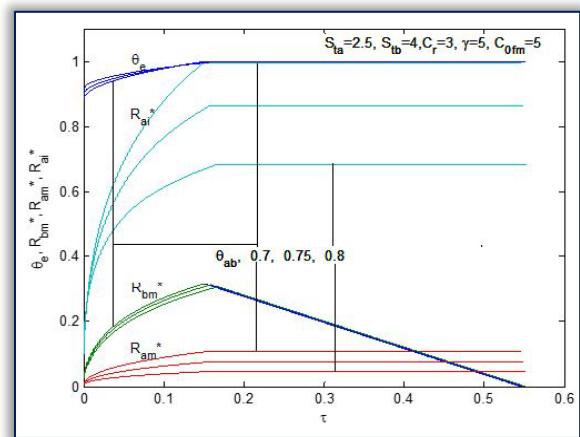


Figure-7: Time variant freezing and melting of bath material R_{bm}^* , onto the additive and associated melt depth, R_{am}^* , of additive, heat penetration depth R_{ai}^* in the additive and the surface interface temperature, θ_e , for different values of melting temperature ratio θ_{ab} , in case of specified values of S_{ta} , S_{tb} , γ , C_r and C_{ofm} .

- C_{ofm} Modified conduction factor, $1/Bi(\theta_b-1)$
- C_p specific heat, $(J Kg^{-1}K^{-1})$
- C_r heat capacity ratio, Cb/Ca
- h heat transfer coefficient, $Wm^{-2} K^{-1}$
- L latent heat of fusion, JKg^{-1}
- T_b bulk temperature of the bath material, K

R_{ah} non-dimensional radius in the heat penetration region of the additive, (r_{ah}/r_a)

R_{ai} non-dimensional radius of the heat penetration front in the additive at any

SUBSCRIPTS

a cylindrical additive,

ai initial condition of additive,

af within melting or freezing region of additive,

ah within heating region of additive,

am melting or freezing of additive,

b frozen bath material or bulk condition of bath material,

bf within melting or freezing region of bath material,

bm melting or freezing condition of bath material, (r_{bf}/r_b)

R_{bf} non-dimensional radius within the frozen layer region, (C_{brbf}/C_{ba})

R_{bm} non-dimensional radius of the frozen layer front at anytime, (C_{brbm}/C_{ba})

S_{ta} Stefan number of the additive, $Ca(T_{am}-T_{ai})/L_a\rho_a$

S_{tb} Stefan number of the bath material, $C_b(T_{bm}-T_{bi})/L_b\rho_b$

t time, s

T temperature, K

T_e instant equilibrium temperature at the interface between the additive and the frozen layer, K

GREEK LETTERS

α thermal diffusivity, $m^2 s^{-1}$

γ property ratio, $(K_b C_b / K_a C_a)$

ρ density, $(Kg m^{-3})$

θ non-dimensional temperature, $(T - T_{ai}) / (T_{bm} - T_{ai})$

τ non-dimensional time, $(K_b C_b / Ca^2 r_0^2) t$

SUBSCRIPTS

a cylindrical additive,

ai initial condition of additive,

af within melting or freezing region of additive,

ah within heating region of additive,

am melting or freezing of additive,

b frozen bath material or bulk condition of bath material,

bf within melting or freezing region of bath material,

bm melting or freezing condition of bath material,

References

- [1] Singh R.P., Prasad A., 'Integral model based freezing and melting of a melt material onto solid additive.' *Mathl. Comput. Modeling*, 2003, Vol.37, pp.849-62.
- [2] Kruskopt A., 'A model for scrap melting in steel converter', *Metall Material Trans.B* Vol.46, No.3 pp.1-27.
- [3] Sanyal S., Chandra S., Kumar S., Roy G.G. 'An improved model of cored wire injection in steel melt.' *ISIJ, International*, 2004, Vol.44, pp.1157-65.
- [4] Singh U.C., 'Ph.D. thesis 2014, Birla Institute of Technology, Mesra, Ranchi, India.
- [5] Li G., Brooks G., Provatas N. 'Kinetics of scrap melt in liquid steel.' *Metall. Trans.B*, 2005 Vol. 36B, pp.293-302.
- [6] Pendelaers L., Verhaeghe F., Barrier, Gardin D.P., Wollants P., Blanpain B., 'Theoretical evaluation of influence of convective heat transfer and original sample size on shell melting time during Titanium dissolution in secondary steel melting.' *Ironmaking Steelmaking*, 2010, Vol.37, pp.516-21.
- [7] Pendelaers L., Verhaeghe F., Blanpain B., Wollants P., Gardin P., 'Interfacial reaction during Titanium dissolution in liquid iron. A combined experimental and modeling approach.' *Metall. Trans.B*, 2009 Vol. 40B, pp.676-684.
- [8] Argyropoulos S.A and Guthrie R.I.L., 'The Dissolution of titanium in liquid steel.' *Metale. Trans. B*, 15 (1), B, 47-58 (1984).
- [9] Argyropoulos S.A and Sismansis P.G., 'The Solution kinetics of zirconium in liquid steel.' *Steel Research*, 68(8), 345-354 (1997).
- [10] Penz F.M., Schenk J., Ammer R., G. Losch K and Pastucha K., 'Dissolution of scrap in hot metal under Linz-Danawitz (D) steel making condition', *Metals*, Dec.2018, Vol.8, pp 1078-87.
- [11] Argyropoulos S.A and Sismansis P.G., 'The Mass Transfer kinetics of Niobium Solution in Liquid Steel.' *Metale. Trans. B*, 22 (4), 417-428 (1991).
- [12] Jiao Q., Themelis N.J., 'Mathematical modeling of heat transfer during the melting of solid particles in liquid slag or melt bath.' *Canadian Metall, Quarterly*, 1993, Vol.32, No.1, pp.75-83.
- [13] Rohmen E., Bergstron T., Engh T.A., 'Mathematical modeling of heat transfer during the melting of solid particles in liquid slag or melt bath.' *INFACON*, Trondheim, Norway, 1995, pp. 683-95.
- [14] Kumar R., Chandra S., Chattrjee A, 'Kinetics of ferroalloy dissolution in hot metal and steel.' *Tata search*, 1997, pp.79-85.
- [15] Taniguchi S., Ohmi M., Ishiura S., Yamauchi S., 'A cold model study of gas injection upon the melting rate of solid sphere in a liquid bath.' *Transactions ISIJ*, 1983, Vol.23, pp.565-70.
- [16] Taniguchi S., Ohmi M., Ishiura S., 'A hot model study of gas injection upon the melting rate of solid sphere in a liquid bath.' *Trasactions ISIJ*, 1983, Vol.23, pp.571-57.
- [17] Li, B.K., Ma X.F., Zhang X.R., He J.C., 'Mathematical model for melting processes of solid particles in metal bath.' *Acta Metallurgica Sinica*, 1999, Vol.12, No.3, pp.259-266.
- [18] Pineda- Martinez, E., Harnandez-Boconeagra, C. Albertto., Conejo, A.N., and Ramirez-Argaez, M.A., 'Mathematical modeling of the melting of sponge iron in a bath of non-reactive molten slag', *ISIJ Int.* 2015, Vol.55, No.9, pp 1906-15.
- [19] Ramirez-Argaez M.A., Conejo A.N. and Lopez-Cornejo M.S., 'Mathematical modeling of the melting rate of metallic particles in the EAF under multiphase flow', *ISIJ Int*, 2015, Vol. 55 No.1, pp 117-125.
- [20] Zhou B., Yang Y., Reuter M.A. 'Modelling of Melting behavior of Aluminum Metal in Molten salt and Melt bath.' *Extraction of processing division meeting of TMS, Luter, Sweden*, 16-20 June, (2002).
- [21] Zhang L., and Oeters F., 'Mathematical modelling of alloy melting in steel melt' *Steel Research*, 70, 128-134 (1999).
- [22] Zhang L, 'Modeling on melting of sponge iron particles in iron bath.' *Steel Res.*, 1996 Vol.67, No.11, pp.466-72.
- [23] Singh U.C., Prasad A., Kumar A., 'Freezing and melting of a bath material onto cylindrical solid additive in an agitated bath.' *J. Min. Metall, Sect B- Metall*, 2012, Vol.48 (1) B, pp.11-23.
- [24] Singh U.C., Prasad A., Kumar A., 'A lump integral model for freezing and melting of a bath material onto a plate shaped solid additive in agitated bath.' *Acta Metallurgica Slovaca*, 2013, Vol.19, No.1, pp. 60-72.
- [25] Singh U.C., Prasad A., Kumar A., 'A lump integral model based freezing and melting of a bath material onto a cylindrical additive of negligible resistance *J. Min. Metall. Sec.B-Metall*, 49, (3), 245-256 (2013).
- [26] Singh U.C., Prasad A., Kumar A. 'Integral model for development of instant interface temperature at time $t = 0^+$ of cylindrical solid additive bath system.' *Metall. Transactions B*, 2011, Vol.42B, pp. 800-06.

- [27] Prasad S., Prasad A., and Kumar A., 'Development of instant interface temperature at time $t=0^+$ of low melting temperature cylindrical solid additive-bath system.' Metall. Material Transactions B, 2015, Vol.46B, No.3, pp.2616-17.
- [28] Singh R.P., Prasad A., 'Mathematical model for instant interface equilibrium temperature at time $t=0^+$ of solid additive-melt bath system.' Ironmaking and steelmaking, 2005, Vol.32, pp.411-17.
- [29] Singh R.P., Prasad A., 'Freezing and melting of an agitated bath material onto a plate additive with its temperature-dependent heat capacity, In the proceeding of the 7th European Oxygen Steel making Conference Trinec, Czech Republic, 2014, Sept.9-11.
- [30] Singh R.P., Prasad A., 'Freezing and melting of a bath material onto a negligible thermal resistance plate additive having its heat capacity temperature-dependent' In the proceeding of the 6th international conf. on modeling and simulation on metallurgical processes in steel making. Bardolino, Garden lake, Italy, 2015, Sept. 23-25.
- [31] Sismansis P.G. and Arigropoulos S.A., 'Modelling of Exothermic Dissolution Canadian Metall, Quarterly, 1988, Vol.27, No.2 pp.123-133.
- [32] Arigropoulos S.A., Guthrie R.I.L., "Dissolution kinetics of ferro-alloys in steel making" Proceeding steel making conference, 65, 1982, pp 156-167.
- [33] Epstein M. and Hauser G.M., 'The melting of finite steel slabs in flowing nuclear reactor fuel.' Nucl. Eng. Des., 1979, vol. 52, pp. 411-28.
- [34] Prasad A. and Singh S.P., 'Conduction controlled phase change energy storage with radiative heat addition.' Trans. ASME, 1994, vol. 166, pp. 218-23.
- [35] Prasad A., 'Radiative melting of materials with melt removal.' J. Spacecraft and Rockets: 1980, vol.17, pp. 474-477.
- [36] Myers T.G., Mitchell S.L., Muchabibaya G and Myers M.Y., 'A cubic heat balance intergral method for one dimensional melting of a finite thickness layer' Int. J. Heat Mass Transfer, 2007, Vol.50, pp. 5303-17.
- [37] Carslaw H.S. and Jaeger J.C., 'Conduction in solid,' Oxford University press, N.Y., 1959, page.72.
- [38] Chung B.T.F. and Yeh L.T., 'Solidification and melting of material subject to convection and radiation.' , Journal space craft, 1975, Vol.12, No.6, pp. 329-33.
- [39] Yeh L.T and Chung B.T.F., 'Phase change in radiative and convecting medium with variable thermal property.', Journal space craft, 1977, Vol. 14, No.3, pp. 178-82.
- [40] Lardner T.J., 'Approximate solution of phase change problem.' AIAA Journal, 1967, Vol.5, No.11, pp.2079-80.
- [41] Prasad S., Prasad A., Kumar A., 'Axisymmetric freezing and melting of an agitated bath material around a low melting temperature cylindrical additive' Annals of Faculty Engineering, Romania, May2018, pp53-66.
- [42] Prasad S., Prasad A., Kumar A. "Axisymmetric Freezing and Melting of a Bath Material onto a Low Melting Temperature Cylindrical Solid Additive of negligible Thermal Resistance." Under consideration, in la metallurgia Italiana.



ISSN 1584 – 2665 (printed version); ISSN 2601 – 2332 (online); ISSN-L 1584 – 2665
copyright © University POLITEHNICA Timisoara, Faculty of Engineering Hunedoara,
5, Revolutiei, 331128, Hunedoara, ROMANIA
<http://annals.fih.upt.ro>